Defense Technical Information Center Compilation Part Notice

ADP012205

TITLE: Production and Magnetic Properties of Nanocomposites Made of Ferrites and Ceramic Matrices

DISTRIBUTION: Approved for public release, distribution unlimited

This paper is part of the following report:

TITLE: Nanophase and Nanocomposite Materials IV held in Boston, Massachusetts on November 26-29, 2001

To order the complete compilation report, use: ADA401575

The following component part numbers comprise the compilation report:
ADP012174 thru ADP012259

Mat. Res. Soc. Symp. Proc. Vol. 703 © 2002 Materials Research Society V5.9

PRODUCTION AND MAGNETIC PROPERTIES OF NANOCOMPOSITES MADE OF FERRITES AND CERAMIC MATRICES

H. A. CALDERON[1], A. HUERTA[1], M. UMEMOTO[2], K. CORNETT[3]
1 Depto. Ciencia de Materiales ESFM-IPN, Apdo. Postal 75-707, México D.F. 07300
2 Dept. Production Systems, Technical Univesity of Toyohashi, Japan
3 Motorola Inc. Fort Lauderdale FLA, USA.

ABSTRACT

This investigation deals with the production of materials containing a dispersion of magnetic nanoparticles in an insulating matrix. Such a distribution of magnetic centers is expected to absorb electromagnetic radiation in a range of wavelengths. Wüstite-magnetite and magnesia-magnesioferrite nanocrystalline ceramics have been prepared by mechanical milling and spark plasma sintering. As-milled powders have a nanocrystalline structure in both systems. Low energy milling gives rise to an increasingly higher volume fraction of wüstite as a function of milling time in the $Fe_{1-x}O$-Fe_3O_4 system. Similar results are obtained in the MgO-$MgFe_2O_4$ system with increasingly larger amounts of $MgFe_2O_4$ produced by milling. Composites of magnetic particles (Fe_3O_4 or $MgFe_2O_4$) in a nonconductive matrix (FeO or MgO, respectively) are found in the sintered samples. Measurement of magnetic properties can be used to determine conclusively the nature of the developed phases and the effect of grain size.

INTRODUCTION

Materials for absorption of electromagnetic waves can be divided into basically two types. One of them consists of pure materials such as ferrites and the other is typically a composite including a polymeric supporting phase and a magnetic material in dispersion or forming a characteristic arrangement. Ferrites have high potential for electromagnetic wave absorption since they have frequency dependent physical properties such as permittivity and permeability. There are several investigations on the frequency dispersion of complex permeability in polycrystralline ferrite [1-3]. Such properties depend on the chemical composition of the ferrite and on the postsintering density, grain size, porosity and inter or intragranular porosity [3]. On the other hand, composite wave absorbers are also commonly produced. Takada et al. [4] report the properties of a Ferrite/SiC sintered composite showing a dependence between the volume fraction of ferrite and the absorption properties. Arrangements of aligned thin magnetic metal particles in polymers have also been successfully used as electromagnetic wave absorbers [5]. Nevertheless few efforts have been made to evaluate the effect of a nanostructure (including grain size and scale of the magnetic centers) on the wave absorbing properties of this type of materials. This investigation deals with the production of a wave absorber by using mechanical milling. Such an experimental method produces nanostructured materials usually in a non stable condition but proper heat treatment can be used to achieve the desired dispersion of nanomagnetic particles in the insulating matrix. This report summarizes the production, magnetic properties and characterization of materials designed for electromagnetic wave absorption.

EXPERIMENTAL PROCEDURE

Materials containing particles of $MgFe_2O_4$ (magnesioferrite) in a $Mg_{(1-x)}Fe_xO$ (magnesio-wustite) matrix and particles of Fe_3O_4 (magnetite) into Fe_xO (wustite) have been produced by the mechanochemical reaction of pure components in low, high and ultrahigh energy mills (horizontal, planetary and Spex mills, respectively). All powder handling was performed in an

Ar-filled glove box with an oxygen content below 0.01 ppm. Consolidation of powders was performed by spark plasma sintering (SPS). Cylindrical solid samples of 18 mm or 13 mm in diameter and 5 mm of thickness were produced by sintering at high temperature (873 to 1273 K) and low pressure (50 MPa) or at low temperature (673, 773 K) and high pressure (100 MPa). Microstructural characterization was done by means of X-Ray diffraction (Siemens D-500, $Cu_{K\alpha}$ XRD), scanning electron microscopy (JSM-200, SEM), transmission electron microscopy (Hitachi 800, TEM) and high resolution electron microscopy (Philips CM300, HREM). Measurement of magnetic properties was made in a vibrating sample magnetometer (Riken Denshi Co., VSM). Identification of the iron containing phases was made by Mössbauer spectroscopy (Source Co-60, MöS).

RESULTS AND DISCUSION

XRD patterns of powders in the Fe_xO-Fe_3O_4 system milled in a horizontal mill indicate a reduction of grain size and a variation of the unit cell dimensions. Fig. 1a shows the XRD of different samples milled for 1000 h. A variety of starting materials has been used, pure Fe_3O_4, Fe_3O_4 with additions of Fe or C and Fe_2O_3 together with Fe. The obtained XRD patterns have broad intensity maxima at similar angular positions suggesting the formation of the same phases in all cases. The angular positions expected for the pure phases are also indicated in the lower section of this figure. It can be seen that the experimental angular positions do not correspond to either of the equilibrium phases (Fe_xO, Fe_2O_3 or Fe_3O_4). They are close to wustite or magnetite and thus the experimental peak positions can be interpreted either as a Fe-lean non-equilibrium wüstite phase or as a Fe-rich non-equilibrium magnetite. However, consideration of the peak displacements suggests that an Fe-lean wüstite is formed during milling with some minor amounts of magnetite. The MgO-$MgFe_2O_4$ system is represented in Fig. 1b that shows XRD patterns corresponding to the sample MgO-4 cat.% Fe after different milling times. The mixture was prepared with powders of Fe_2O_3 and MgO as starting materials. Fig. 1b shows that low amounts of Fe_2O_3 can be dissolved into the MgO lattice producing lattice distortions that give rise to variation of the expected angular positionso of MgO. The displacement is always towards large lattice spacing and thus it is likely that the MgO lattice saturates with Fe and thus the as-milled microstructure is composed mostly of $Mg_{1-x}Fe_xO$. Other peaks indicate the presence of $MgFe_2O_4$, especially after long milling times. The XRD maxima in the patterns also show broadening indicating a reduction of the crystal size.

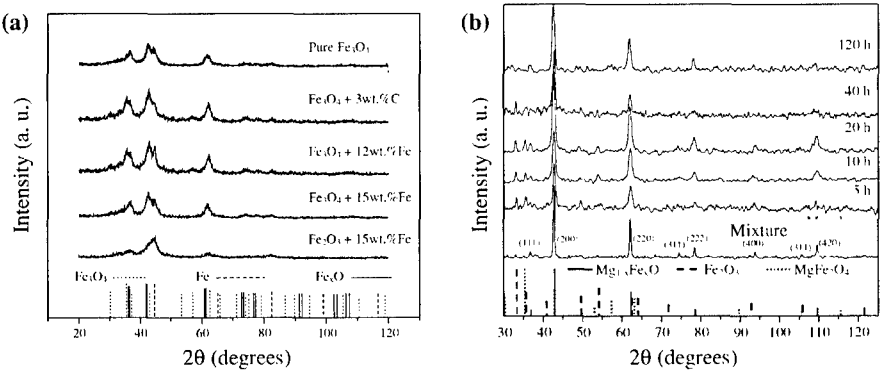

Figure 1. XRD patterns of powders after milling 1000 h in a horizontal mill from the Fe_xO-Fe_3O_4 system. (b) XRD patterns of MgO-4cat.% Fe before and after milling in a Spex mill.

Figure 2 shows a typical view of the grain structure of the as-milled powder particles. In this case the sample is Fe_3O_4 with addition of 12 wt.% Fe after 200 h of milling. Nanosized grains can be clearly seen with an average size of 10 ± 8 nm (Fig. 2a). The corresponding diffraction pattern is given in Fig. 2b, the somewhat diffuse rings are typical of fine grained materials and the angular positions allow identification of the phases Fe_3O_4 and Fe_xO.

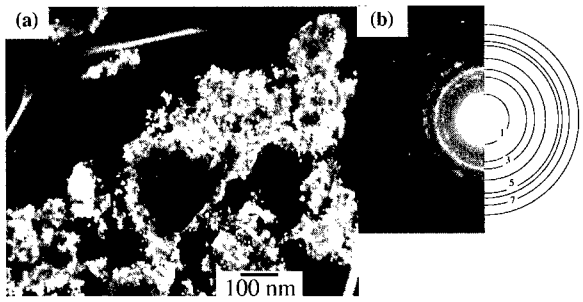

Ring	Fe_3O_4	Fe_xO
1	(111)	
2	(220)	
3	(222)	(111)
4		(200)
5	(422)	
6	(511)	
7	(440)	(220)
8	(533)	(311)

Figure 2. (a) Dark field TEM image of sample Fe_3O_4+12 wt.%Fe milled in a horizontal mill for 200 h. It was taken with the overlapping reflections (222) of Fe_3O_4 and (111) of Fe_xO. (b) Diffraction pattern.

Mössbauer spectroscopy (MöS) has been used to identify the nature of the iron-containing phases. Fig. 3a shows an example that corresponds to pure Fe_3O_4 milled for 500 and 1000 h in a horizontal mill. They consist of two separate sextets (magnetic effect, see *i* and *ii*) and one pair of overlapping doublets (paramagnetic effect, see *I* and *II*). Thus only two phases can be identified i.e., magnetite and wüstite. The spectra exhibit a magnetic relaxation as a function of the milling time i. e., the intensity of the sextets (magnetite phase) is smaller for the sample milled for 1000 h and therefore the amount of $Fe_{1-x}O$ increases with longer milling times. Quantitative evaluation shows an increase from 66.6 % to 74 % for 500 and 1000 h of milling. In addition, the spectra present a strong absorption asymmetry, which can be related to disordered phases or nanosized grains. These results suggest that during milling magnetite transforms into wustite. The same tendency, i.e. formation of a solid solution, is found for the other investigated mixtures. Figure 3b shows the MöS spectra of MgO - 4 cat.% Fe milled for 40 and 120 h in a Spex mill. The spectrum of the sample milled for 40 h consists of two sextets (magnetic effect, see *i*) and two doublets (paramagnetic effect, see *ii*). The magnesiowüstite ($Mg_{1-x}Fe_xO$) phase produces the two doublets and the magnesioferrite ($MgFe_2O_4$) the two sextets in the MöS spectrum. Quantitative evaluation shows that the as-milled powders are rich in magnesioferrite (75% refered to the total amount of Fe-containing phases) with low amounts of magnesiowüstite. On the other hand, the spectrum of the sample milled for 120 h consists of one sextet (see *I*), two doublets (see *II*) and one singlet (see *III*). The doublets are related to magnesiowüstite (a total content of 80 %) and the sextet is due to pure iron (20 %). These results suggest that the mechanochemical reaction between MgO and Fe_2O_3 ends before 120 h of milling and also that the magnesioferrite formed at shorter milling times (40 h) transforms into magnesiowüstite if milling is continued further. Measurement of magnetic properties of as-milled powders also indicates the formation of a new magnetic phase during milling i.e., magnesioferrite. Thus a similar transformation sequence is observed in this system in that the spinel oxide precedes the formation of the solid solution i.e., $MgO+Fe_2O_3 \rightarrow MgO+MgFe_2O_4 \rightarrow Mg_{(1-X)}Fe_XO$.

Figure 4 shows measurements of magnetization (M) as a function of applied field (H) in the wüstite-magnetite system after mechanical milling in a horizontal mill. Measurements of samples

containing magnetite as starting material show a decrease of saturation magnetization M_s as a function of milling time. A different behavior is observed in the sample prepared with hematite as shown in Fig. 4a (Fe_2O_3 + 15 wt.% Fe), where Ms shows a fluctuation in value. The monotonic

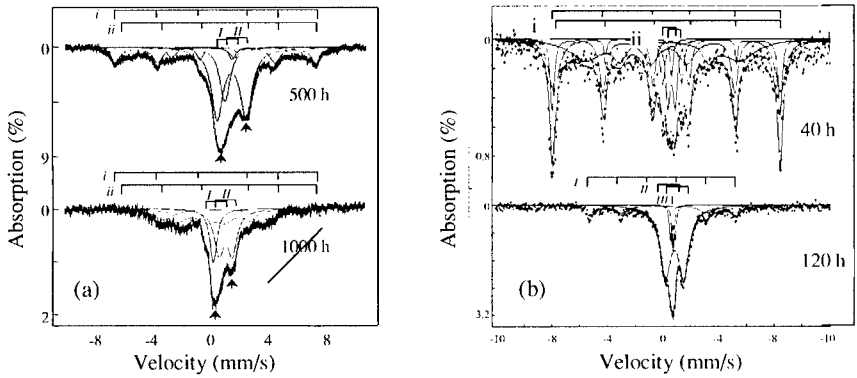

Figure 3. MöS spectra. (a) Pure Fe_3O_4 milled 500 and 1000 h in a horizontal mill. (b) MgO-4 cat.% Fe powders milled 40 and 120 h in a Spex mill.

reduction in M_s can be seen in Fig. 4b (M_s Vs milling time) that shows a summary of results for the as-milled powders. Such a trend can be explained by the transformation of magnetic phases into non-magnetic phases i.e., magnetite and/or iron into wüstite. A net reduction of approximately 50% in Ms is seen when comparing M_s values after 50 and 1000 h of milling. However, the transformation of magnetic phase into paramagnetic wüstite is not complete even after 1000 h of milling due to the applied low energy processing. A different behavior is seen for the sample prepared with Fe_2O_3 as starting material. There is an increase of the M_s value for milling times up to 500 h. Additional milling promotes M_s values similar to those found for other samples. Apparently Fe_2O_3 first transforms into Fe_3O_4 upon milling and then to Fe_xO. Therefore the decomposition sequence appears to be $Fe+Fe_2O_3 \rightarrow Fe_3O_4 \rightarrow Fe_xO$. This can also be predicted from the relative values of the oxides free energy of formation [6]. Thus the initial components have a definite influence on formation of phases during milling. On the other hand, the central sections of the hysteresis loops are magnified and shown in the insert of Fig. 4a. This can be used to evaluate the coercivity of the as-milled powders (half width of hysteresis loop with no induced field, M). As seen in Fig. 4a, the coercivity remains constant in this sample as a function of milling time, indicating that the size of the magnetic domains is independent of such a variable.

Figure 5 shows representative measurements of magnetic properties in sintered samples. Fig. 5 corresponds to pure Fe_3O_4 milled for 500 and 1000 h and sintered at 1073 and 1173 K. Lower saturation magnetization values are achieved in these samples with respect to the as-milled powders (see Fig. 4b). This suggests that a phase transformation takes place during the sintering process, most likely a transformation to oversaturated wüstite (paramagnetic) which represents the solid solution of Fe and O. This phase can still transform upon aging to wüstite and magnetite in metastable equilibrium as shown in [7] for materials prepared by conventional melting techniques. In addition the relative differences among the curves shown in Fig. 5 can be explained on the basis of two effects i.e., the magnetic domain size (s_m) and the volume fraction of magnetite (f_v). A higher f_v of magnetite produces a higher M_s value while a smaller s_m gives rise to a higher coercivity. The central sections of the hysteresis loops have been magnified and are shown in the insert in to to depict the differences in coercivity.

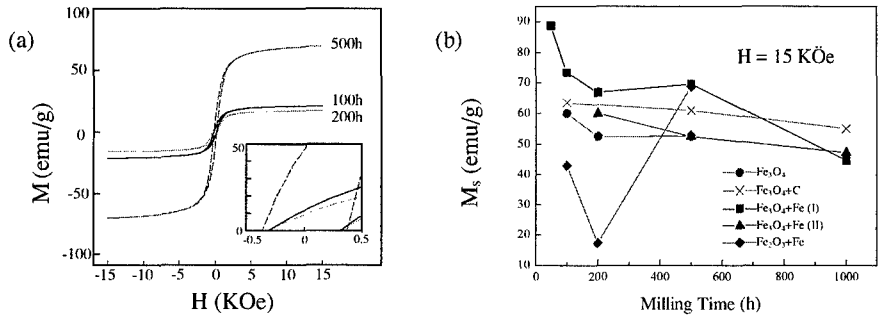

Figure 4. Magnetization curves of wüstite magnetite system after milling in a horizontal mill. (a) Fe_2O_3 + 15 wt.% Fe. (b) Saturation magnetization (M_s) as a function of the milling time.

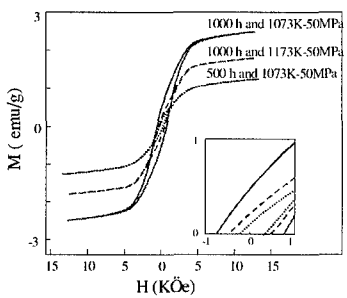

Fig. 5. Magnetization curves of sintered Fe_3O_4 samples.

Thus for example the sample milled for 1000 h and sintered at 1073 K contains a finer distribution of magnetic particles in the paramagnetic Fe_xO matrix. However in all cases in Fig. 5, the formation of a fine dispersion of magnetic particles in a matrix of Fe_xO is evident. Therefore it is possible to control the magnetic behavior by controlling the milling time and the sintering temperature.

The final microstructure after SPS depends on the sintering conditions. Low sintering temperatures produce microstructures composed of fine nanograins around 30 nm in average size and very similar to the microstructures of as-milled powders. SPS at 1073 K gives rise to equilibrium phases in most cases. In addition, the grain size depends on the processing temperature. For example powders of pure Fe_3O_4 milled for 1000 h produce an average size of 230 ± 120 nm if sintered at 1173 K while a value of 150 ± 70 nm is found for sintering at 1073 K. In general sintering below 1073 K allows retention of the nanocrystalline grain structure.

As sintered samples have a characteristic dispersion of phases. Fig. 6 shows darks field images and diffraction patterns of some grains in a sample sintered at 1273 K after 500 h of milling with a nominal composition of Fe_3O_4 with 15 wt.% Fe. The images have been obtained in dark field by using the satellite reflections of the diffraction patterns. The modulated microstructures are typical of an spinodal decomposition process (see arrows). Nucleation by an spinodal mechanism is rarely seen in ceramic phases and it can appear in this wustite – magnetite system among other factors because of the close structural similarities between the two lattices. The oxygen sublattice is common in the two lattices giving a perfect coherency between the two phases and only the Fe content changes to produce the typical composition modulation on the spinodal decomposition. The microstructure formed during sintering has been also observed by means of HREM. Fig. 7 shows experimental and processed images of the sample Fe_3O_4-15wt. % Fe milled for 200 h and sintered at 1173 K. Two different orientations are given in this figure i.e., [100] and [110] as shown in the inserted diffraction patterns obtained from a Fourier transform of the experimental image. The experimental images (Figs. 7a and 7c) show the presence of domains where different spacings of the structural lattice are apparent. Such domains can be seen more easily in the

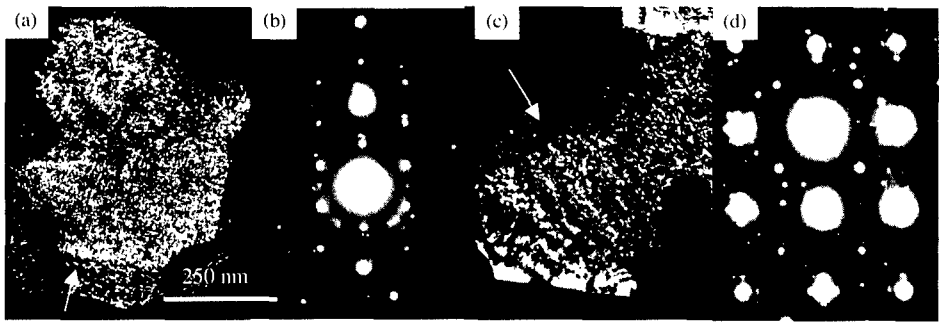

Figure 6. TEM images from Fe_3O_4-15wt.% Fe milled for 500 h and sintered at 1273 K. (a) and (c) Dark field images form [200] reflections. (b) and (d) Electron diffraction patters showing satellite reflections.

processed images. The processing consists in creating a Moire pattern with a selected reflection from the diffraction pattern. The differences (if any) in the periodic distribution created by domains nucleated independently as in the case of an spinodal decomposition can then be more easily observed.

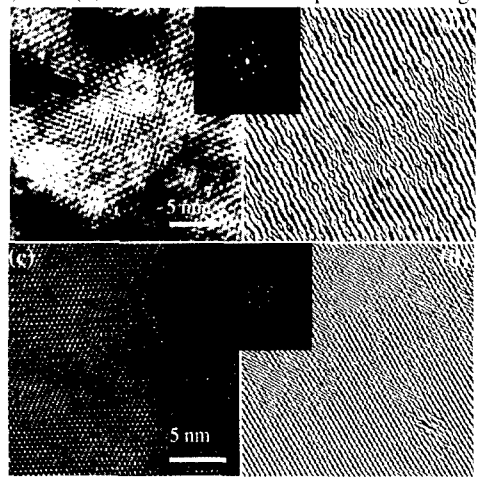

Figure 7. Fe_3O_4-15wt. % Fe milled for 200 h and sintered at 1173 K. (a) HREM image with B = [100]. (b) Moire pattern of image a. (c) HREM image with B = [110]. (d) Moirè pattern of image c.

CONCLUDING REMARKS

A fine distribution of magnetic particles in a nonconductive matrix can be produced by mechanical milling and sintering in the systems Fe_xO-Fe_3O_4 and MgO-$MgFe_2O_4$. It is noticed that phase formation is related to the relative values of the energy of formation. The spinel phase precedes the formation of the oxygen solid solution in both systems under investigation.

ACKNOWLEDGEMENTS

AH acknowledges financial support from CONACYT and TUT. HAC acknowledges support from CONACYT (Project 28925 U), Motorola Inc. and COFFA-IPN. NCEM-LBNL is gratefully acknowledged for the use of HREM equipment.

REFERENCES

1. G.T. Rado, Rev. Mod. Phys. 25, 81 (1953).
2. D. Polder and J. Smit, Rev. Mods. Phys. 25, 89 (1953).
3. T. Nakamura, J. Appl. Phys. 88, 348 (2000).
4. J. Takada, M. Nakanishi, M. Yoshino, T. Fuji, M. Fukuhara, A. Doi, Y. Kusano, Adv. Powder Metal. and Part. Mats, Pub. by Metal Powder Ind. Fed., Part 12, p. 11 (1999).
5. M. Matsumoto and Y. Miyata, IEEE Trans. on Mag., 33 (1997) 4459.
6. C.H.P. Lupis, *Chemical Thermodynamics of Materials*, Prentice-Hall Inc. A Simon and Schuster Company, Englewood Cliffs, New Jersey, (1983).
7. M. E. Fine, American Ceramic Society Bulletin, 51 (1972) 510-15.